^{1}H NMR Imaging and Spectroscopy Studies of the Polymerization of Acrylamide Gels

S. Ahuja,* S. L. Dieckman,* N. Gopalsami, and A. C. Raptis

Energy Technology Division, Sensors, Instrumentation, and Nondestructive Evaluation Section, Argonne National Laboratory, Argonne, Illinois 60439-4825

Received February 12, 1996; Revised Manuscript Received May 9, 1996[⊗]

ABSTRACT: ^{1}H nuclear magnetic resonance spectra and images have been acquired during polymerization of a mixture of soluble reactive methacrylamide (monomer) and *N*,*N*′-methylenebisacrylamide (cross-linking molecule). The mixture was polymerized by adding ammonium persulfate (initiator) and tetramethylethylenediamine (accelerator) to form long-chain, cross-linked polymers. Study of the time-varying spin−lattice relaxation times (T_1) during the polymerization was conducted at 25 and 35 °C and the variation of spectra and T_1 with respect to the extent of polymerization was determined. To verify homogeneous polymerization, multidimensional ^{1}H NMR imaging was utilized for in-situ monitoring of the process. The intensities from the images are modeled and the correspondence shows a direct extraction of T_1 data from the images.

Introduction

Development of the ability to control and design the physical and chemical properties of polymeric materials continues to be an active area of technology. Advancement in this field depends, in part, on an increased understanding of the molecular origins of macroscopic behavior. Relaxation of the nuclear-spin system as it gives up energy to its environment typically takes place on a time scale of 0.1 ms to tens of seconds. This time scale can easily be measured via NMR techniques, thus providing the opportunity to externally probe a spin system in various useful ways.[1] NMR imaging techniques have provided information about chemical composition, molecular structure, bonding, molecular interactions, diffusion, mobility, chemical kinetics, flow, etc. and have been employed on many materials including polymers, rubbers, rocket propellants, porous media, coal, wood, and ceramics. NMR imaging can also be used to obtain spatial variations in the physical and chemical properties of materials.[2−5]

Copolymerization of methacrylamide (MAA) and *N*,*N*′-methylenebisacrylamide (MBAA) has been of interest in making strong, machinable polymeric parts.[6] Both aqueous (water-based), as in traditional ceramic processing, and nonaqueous (organic solvent based) versions of MAA−MBAA copolymerization have been studied. The gel-casting slurries are prepared with premixed MAA−MBAA, alumina powder, and the dispersant, Darvan C. Ammonium persulfate (AP) is used as an initiator, and tetramethylethylenediamine (TEMED) acts as an accelerator. The slurry is poured into a preheated mold, allowed to solidify into a formed part, and then dried to remove the solvent (water).[6,7] In the aqueous process, polymerization begins only by the addition of AP and TEMED and the shelf life of the raw premix is longer than that of its nonaqueous counterpart. Study of the nuclear spin relaxation effects in the polymeric network directly correlates with the polymerization process. This article is concerned with the process of aqueous polymerization because the use of water as a solvent facilitates drying and disposal while reducing overall viscosity.

There has been a wide interest in studying polymerization of acrylamides. High-resolution ^{1}H NMR spectroscopy has been used to study the cross-linking polymerization of acrylamide (AA) and MBAA to measure the composition of a residual comonomer mixture during and after polymerization.[8] Also, heterogeneity of solidified acrylic monomer films and their molecular dynamics have been investigated.[9] TEMED, used as an accelerator in the present study to form long-chain, cross-linked polymers, has been used as a probe to study diffusion and electrophoresis in polyacrylamide (PA) gels[10] and AP has been extensively used as an initiator.[11] ^{1}H NMR imaging of cross-linked MAA gels has been performed by other researchers.[12] Separately, MBAA has been used as the cross-linking monomer. Cross-linking polymers and polymeric gels have been used extensively because of their chemical and physical properties, which have been determined by applying NMR to study the motional state of water and the polymer network.[13] Low-temperature studies of aqueous solutions of AA and MBAA with AP and TEMED have shown that polymerization of cross-linked PA to form cryogels is complex and involves intricate chemical and physical phenomena. Furthermore, the dynamics of polymerization depend on the thermal history of the sample.[14] In this work, multidimensional nuclear magnetic resonance (NMR) imaging was conducted to characterize polymerization homogeneity and because in-situ study of the polymerization process was necessary. The varying relaxation effects, especially the spin−lattice relaxation time, T_1, in the premix have been determined by NMR spectroscopy.

Experimental Aspects

High-resolution NMR spectrometry of an MAA−MBAA copolymer mix was performed on a Bruker AM-300 spectrometer with a commercial probe at a magnetic field strength of 7.1 T. Low-resolution NMR spectroscopy and imaging studies were conducted on a Tecmag NMR Kit II and Libra data acquisition system interacting with a CXP-100 spectrometer and a Macintosh Quadra 950 computer. Spectra and images at a magnetic field strength of 2.35 T were obtained by an in-house-built imaging accessory[15] tuned to the proton resonance frequency of 100.13 MHz. Orthogonal linear magnetic field gradients across the specimen were driven by three 1000-W Techron audio amplifiers. A sequence of spectra was acquired with varying interpulse delay times, τ. Delay times of 2, 5, 20, 50, 200, and 500 ms and 2, 5, 10, and 20 s were used in the sequence to obtain 2-D images. For each time delay, the

* To whom correspondence should be addressed.

[⊗] Abstract published in *Advance ACS Abstracts,* June 15, 1996.

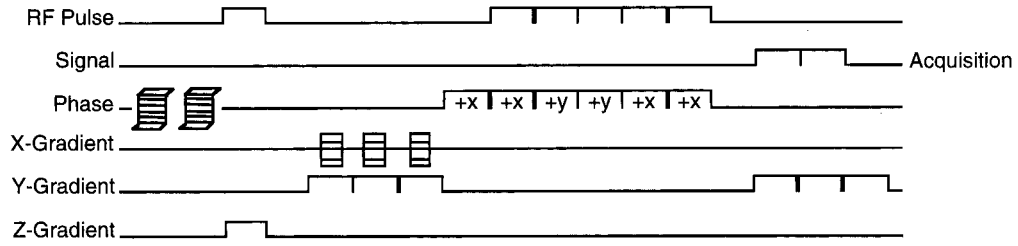

Figure 1. T_1 inversion−recovery 90°−τ−composite 180° sequence for acquisition of time domain data matrix.

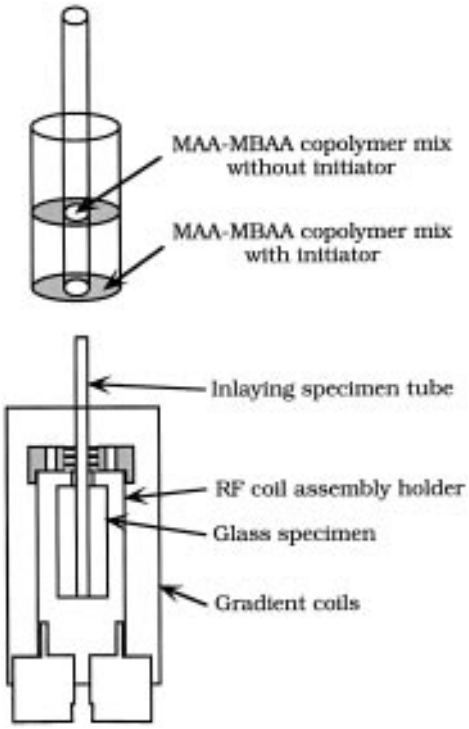

Figure 2. Sample configuration and probe assembly used in imaging experiments.

time domain data matrix of 128 × 128 was obtained by accumulating eight transients. The total time for data acquisition was 139 min. Room-temperature shims were used to acquire a good free induction decay (FID) on a water sample and the measured line width was 28 Hz. The data matrix was made symmetrical by adjusting the gradients, thus obtaining a central image of a slice of a sample cross section.

The samples were prepared from soluble reactive AA (monomer) and MBAA (cross-linking molecules) and the premix was made with water as solvent.[1] The initiator, 10% AP, and the accelerator, TEMED were then added to begin the polymerization of the monomers, which formed long-chain, cross-linked polymers. For high resolution, 5-mm NMR sample tubes were used; for low resolution, the solution was transferred to a 15-mm, cylindrical, flat-bottomed tube and rapidly placed into the probe for spectroscopy experiments.

NMR imaging was conducted on MAA−MBAA prepared in water. During imaging, the obtained NMR signal was largely due to water in the premix and it overwhelmed the signal due to other constituents in the premix. A T_1 inversion recovery sequence 90°−τ−composite 180°, given in Figure 1, indicates delays and gradient activation at specific intervals. For low-resolution imaging experiments, it was necessary to obtain a corresponding contrast between the polymerized and nonpolymerized specimens. For this reason, the sample geometry shown in Figure 2 was such that MAA−MBAA without the initiator was placed in a small-diameter inner tube (5 mm) immersed in a larger diameter (15 mm) tube that contained polymerizing MAA−MBAA and the initiator. The time of the initial measurement was recorded and careful monitoring of the polymerization was conducted with respect to time. Times

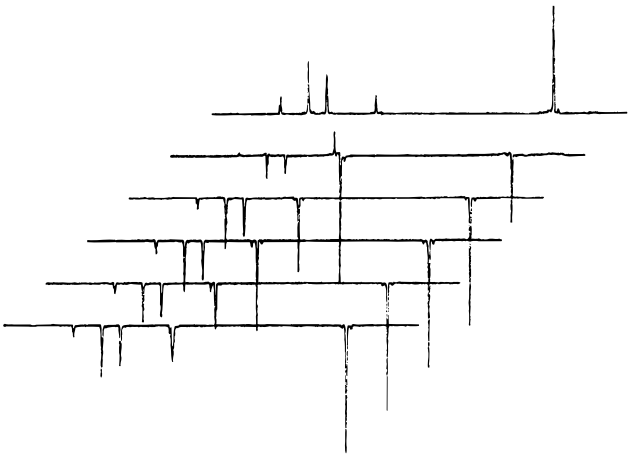

Figure 3. In-situ 2-D stack plot of ^{1}H NMR T_1 inversion−recovery sequence of MAA−MBAA copolymer premix. Spectra acquired at 35 °C at onset of polymerization reaction with respect to varying interpulse delays.

were subsequently recorded at the end of an experiment and at the beginning of the next computer-controlled experiment.

Discussion

NMR spectra were studied as a function of the extent of MAA−MBAA polymerization. The ^{1}H NMR spectra were acquired on individual standard MAA−MBAA reagents and on composite copolymer premix reagents. Spectra were acquired with H_2O (as solvent) at ambient temperature and at 35 °C. The standard inversion−recovery NMR pulse technique, employed for the measurement of T_1, utilized a 180° pulse, followed by a time delay, τ, and then another 90° pulse (180°−τ−90°−acquire). In these studies, real-time ^{1}H NMR spectra of the copolymerization reaction were acquired as a function of reaction time. The spectra demonstrated a reduction in methylene and methyl resonances as the polymerization reaction progressed. A variation of the spin−lattice relaxation rates of the components as a function of reaction extent is expected. ^{1}H NMR studies of spin−lattice relaxation time, T_1 were conducted on the individual standard MAA−MBAA copolymer premix at a magnetic field strength of 7.1 T. Spectra were acquired with D_2O as the solvent at 35 °C to suppress the observable solvent resonance. The standard inversion−recovery NMR pulse technique was employed for these studies. A stack plot of the resultant spectra for the copolymer premix is presented in Figure 3. Variations in relaxation times are indicated by the rate of recovery from the inversion pulse and suggest that as the reaction occurs, spin−lattice times are longer.

NMR spectroscopy and imaging procedures were performed at 25 and 35 °C to determine the variation in T_1 and whether the polymerization is homogeneous. Spectra obtained by low-resolution NMR spectrometry showed the effect of polymerization on the intensity of

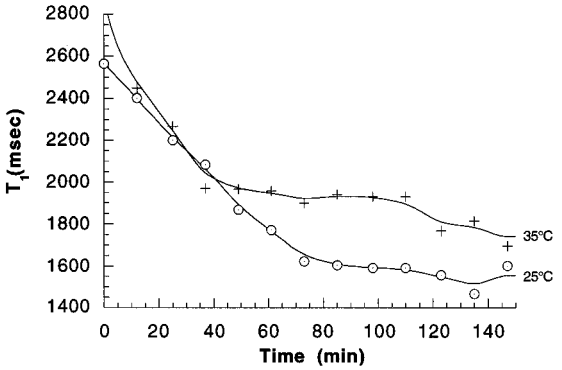

Figure 4. Variation of spin−lattice relaxation time T_1 with time during polymerization of MAA−MBAA at 25 and 35 °C.

the peaks with respect to time at the end of an inversion−recovery sequence. The unchanged peak was identified as that of the solvent, water, although T_1 of the solvent varied as the polymerization progressed. Also, the polymerizing peak encompassed several peaks that were not visible because of low-resolution analysis. Figure 4 indicates the variation of relaxation time during polymerization, derived from inversion−recovery sequence results for the two peaks recorded at 25 and 35 °C. T_1 is a measure of the time taken for transfer of energy to or from the lattice, i.e., for the spin system to approach thermal equilibrium. Large values of T_1, existing at the onset of polymerization in Figure 4, indicate very slow relaxation. The measurements of T_1 reveal the effect of polymerization on the motion of the methyl group and the side and main chains.[16] T_1 measurements can be used to determine changes in molecular motion caused by polymerization.[17,18] In Figure 4, the value of T_1 decreases, depending upon the correlation time of the local motions that contribute to the relaxation. T_1 increases with temperature and decreases during polymerization. This indicates that the polymerization of MAA−MBAA with AP as the initiator and TEMED as the accelerator was more rapid at higher than at lower temperature.

Figure 5 shows a sequence of 2-D ^{1}H NMR images of the MAA−MBAA polymerization reaction with time in the frequency domain. These were obtained by Fourier transforming 2-D spectra initially acquired in the time domain. All of the images show the concentration gradient in the specimen. Figure 5a shows a 2-D ^{1}H NMR image of the MAA−MBAA copolymer premix at 0.0 s. Here, the polymerization has not begun because the initiator and the accelerator have not begun to react with the copolymer premix. During the process, at any temperature, no polymerizing front was observed with imaging techniques and polymer gels formed homogeneously throughout the solution, as seen in the images

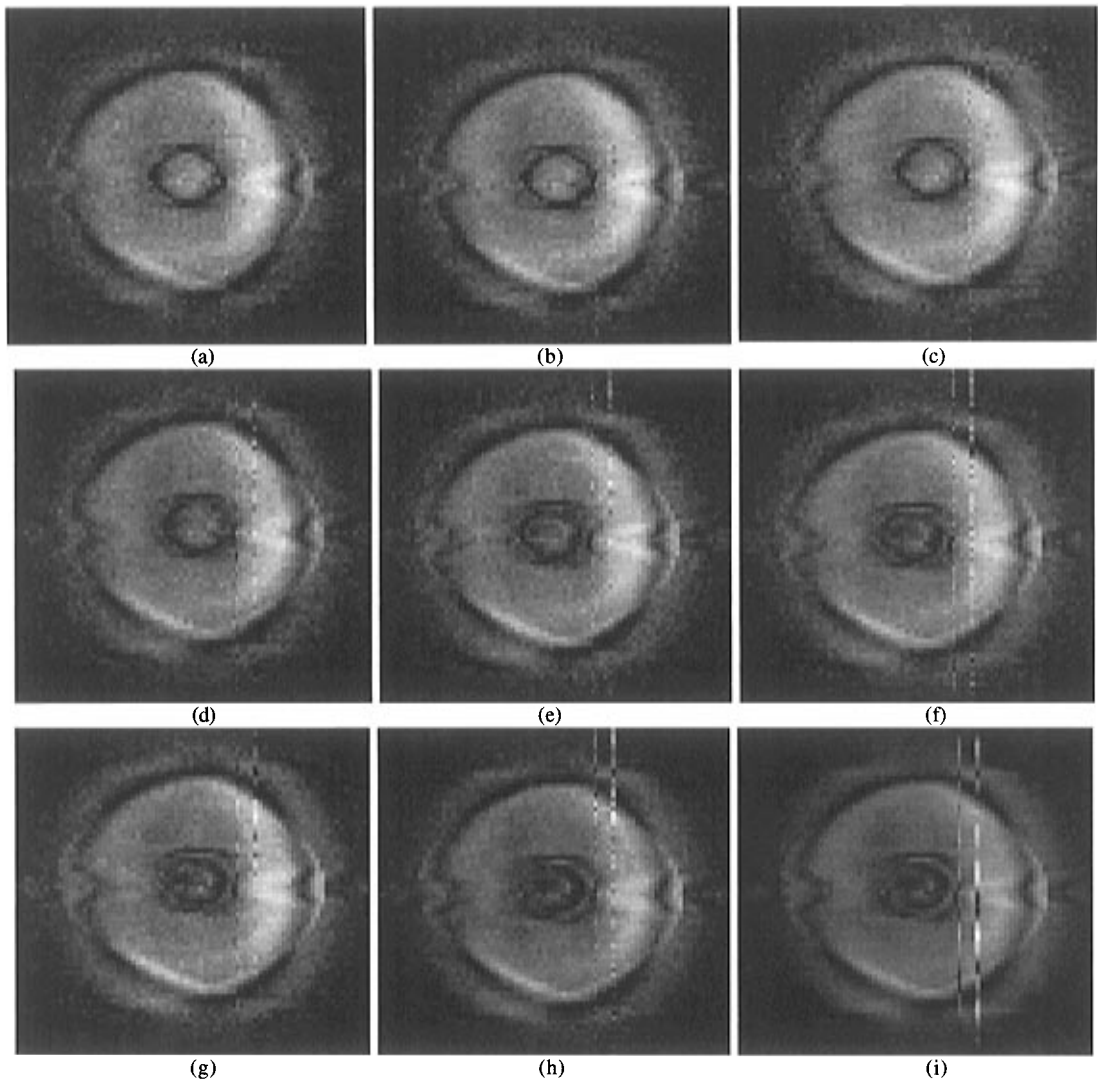

Figure 5. 2-D ^{1}H NMR images at (a) 0, (b) 26, (c) 45, (d) 64, (e) 83, (f) 102, (g) 120, (h) 138, and (i) 157 min of standard MAA−MBAA polymerization reaction with initiator.

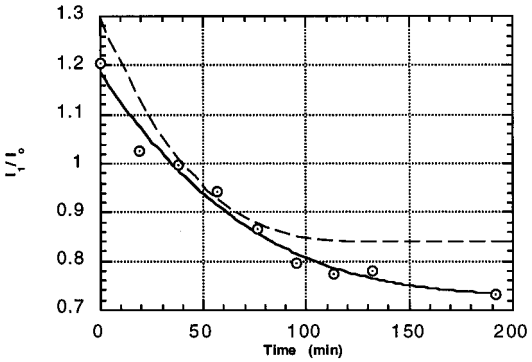

Figure 6. Ratio of intensities of polymerizing MAA−MBAA (I_1) to uninitiated MAA−MBAA (I_0) vs time: solid line, experimental plot derived from images in Figure 5; dashed line, theoretical plot of image intensity according to eq 4.

in Figure 5. It may be noted that the distortion at the periphery of the sample is an artifact of the imaging experiment and relates to the limitation of tuning of the gradient coils in the probe assembly. The sequence of images shows that, because of the polymerization, relaxation occurred more rapidly in the polymerizing MAA−MBAA (i.e., in the outer tube) than in the inner tube where the relaxation remained constant.

Because the images are individually scaled in intensity, it appears that the image intensity of the inner tube decreases. The images also demonstrate the actual time of polymerization. At time 0.0 min, the concentration of the polymerizing specimen in the outer tube was essentially the same as the concentration of the raw specimen without initiator in the inner tube as seen in Figure 5a. As the polymerization continues, the specimen in the outer tube becomes more viscous, which leads to the intermediate intensity shown in Figure 5e at 83 min. Complete polymerization takes place at 139 min as shown in Figure 5i. The intensities of the images did not vary with further acquisition of images. The variation of intensity has been indicated in Figure 6 by a plot (intact line) of the intensity ratio (outside intensity/inside intensity, I_1/I_0) vs time as the polymerization occurred.

The variation in intensity corresponds to that from a simple spherical domain with an exterior sink. If the material is inhomogeneous, the magnetization or intensity decay can be expected to be a composite sum of two exponentials.[19] The curvature in the intensity vs time plot for the MAA−MBAA system strongly indicates that the system is inhomogeneous. Inasmuch as the applied field is larger than the dipolar field, the shape of the decay of this spin−lattice relaxation depends on the small-scale morphology of the inhomogeneities:

$$M(t) = I(t) = \frac{2a^3}{\pi}\sum_{n-1}^{\infty}\frac{1}{2}\exp\left\{-\left[K\left(\frac{n\pi}{a}\right)^2 + \frac{1}{T_1}\right]t\right\} \quad (1)$$

where a is the atomic radius, n is the order, and K is a normalization constant. Magnetization is directly related to the spin-echo intensity; therefore, it is possible to correlate the intensity obtained from the images with the magnetization. Because the fast inversion−recovery pulse sequence was employed to determine T_1, the peak intensity as a function of time, t, can be written as[2,20]

$$M(t) = M_o\{\mathrm{I} - \mathrm{e}^{-D/T_1}\}\mathrm{e}^{-\tau/T_1} \quad (2)$$

where M_0 is a normalization constant, D is the delay time, T_1 is the spin−lattice relaxation time, and the total delay time, τ, is the sum of the individual delays. More accurately, the intensity variation can be verified by using the inversion−recovery sequence and the variation in the spin−lattice and the spin−spin relaxation times as a basis for calculating the image intensities in each voxel. For the standard inversion−recovery NMR pulse technique employed to measure T_1, the images were analyzed to relate the signal intensity to T_1 and the spin−spin relaxation time T_2. The signal intensity is

$$S \propto \rho\mathrm{e}^{-\tau/T_2}(1 - (1 + \mathrm{e}^{-\tau/T_2}))(2\mathrm{e}^{\tau/2T_1} - 1)\mathrm{e}^{-T_1/T_1} + \mathrm{e}^{-\tau/T_2}(2\mathrm{e}^{\tau/2T_1} - 1)\mathrm{e}^{-\tau_{tot}/T_1} \quad (3)$$

where the recovery process is inspected with a 90° pulse applied at time T_I following the inversion and τ_{tot} is the total recovery time. Taking $T_2 \gg \tau$,

$$S \propto (2\mathrm{e}^{\tau/2T_1} - 1)(\rho\mathrm{e}^{-T_1/T_1} + \mathrm{e}^{-\tau_{tot}/T_1}) \quad (4)$$

The relationship in eq 4 shows the codependency of T_1 with the intensity of the obtained images. The dashed line in Figure 6 is the plot of the intensity vs time according to eq 4 for corresponding values of T_1. The decrease in intensity corresponds to the images shown in Figure 5 and the intensity variation (solid line) shown in Figure 6. The theoretical fit according to eq 4 breaks down with further elapse of time because of the assumption that $T_2 \gg \tau$. Because this assumption is only valid for large values of T_2, and therefore large values of T_1, a better fit can be obtained if T_2 is considered in the fitting analysis. This paper has been restricted to variation of T_1. T_2 values were not experimentally determined. Nevertheless, the above analysis demonstrates the capabilities and varying information that can be obtained with NMR imaging techniques. Equation 3 can be used to separately verify the spin−spin relaxation times T_2 if the intensities of the images and T_1 are known.

In future work, we will analyze aqueous gel systems that involve alumina solid loading and composites as well as the concentration differences between the raw specimen and the polymerizing specimen. T_2 values will be determined and the fitting analysis recomputed to understand the differences between eqs 3 and 4. Additional studies are being conducted on the MAA−MBAA system as a function of reaction extent and temperature and as a function of the concentration of individual reactants. This information is expected to provide details on molecular correlation times, sample viscosity, and reaction kinetics. Also, the aqueous organic gel systems that involve the addition of solid particles to the copolymer premix of MAA−MBAA will be imaged and concentration differences will be analyzed to understand how the main quantity of comonomers becomes involved in the polymerization process. Effort is underway to evaluate the potential of NMR imaging to affect development and process control of near-net-shape gel-cast parts. Some of the objectives of the work are to determine the utility of NMR imaging for nondestructive evaluation of voids and flaws in components and for measurement of physical properties, such as the degree of polymerization, viscosity, and specimen strength by correlating these properties with measurable NMR parameters (T_1, $T_{1\rho}$, and T_2).

Acknowledgment. The authors acknowledge the financial support for this work provided by the U. S.

Department of Energy through the Assistant Secretary for Energy Efficiency and Renewable Energy, Office of Transportation Technologies, under Contract W-31−109-ENG-88 and as part of the Ceramic Technology Project of the Materials Development Program, under Contract DE-AC05−84OR21400 with Martin Marietta Energy Systems, Inc. The authors also thank W. A. Ellingson of Argonne National Laboratory and O. O. Omatete of Oak Ridge National Laboratory for support of this project.

References and Notes

(1) McBrierty, V. J.; Douglass, D. C. *J. Polym. Sci.* **1981**, *16*, 295.
(2) Morris, P. G. *Nuclear Magnetic Resonance Imaging in Medicine and Biology*; Clarendon Press: Oxford, U. K., 1986.
(3) Mansfield, P.; Morris, P. G., Eds. *NMR Imaging in Biomedicine*; Academic Press: New York, 1982.
(4) Chein, C.-N.; Hoult, D. I. *Biomedical Magnetic Resonance Technology*; Adam Hilger: New York, 1989.
(5) Dieckman, S. L. *Nondestructive Testing Handbook*, 2nd ed.; Moore, P. O., Ed.; American Society for Nondestructive Testing: Columbus, OH 1995; Vol. 9, p 27.
(6) Omatete, O. O.; Janney, M. A.,; Strehlow R. A. *Am. Ceram. Soc. Bull.* **1991**, *70*, 1641.
(7) Young, A. C.; Omatete, O. O.; Janney, M. A.; Menchhofer, P. A. *J. Am. Ceram. Soc.* **1991**, *74*, 612.
(8) Nieto, J. L.; Baselga, J.; H-Fuentes, I.; Llorente, M. A.; Pierola, I. F. *Eur. Polym. J.* **1987**, *23*, 551.
(9) Voelkel, R. *Solid State NMR of Polymers*; Mathias, L., Ed.; Plenum Press: New York, 1991.
(10) Gibbs, S. J.; Johnson, C. S., Jr. *Macromolecules* **1991**, *24*, 6110.
(11) Hikichi, K.; Ikura, M.; Yasuda, M. *Polym. J.* **1988**, *20*, 851.
(12) Yasunaga, H.; Kurosu, H.; Ando, I. *Macromolecules* **1992**, *25*, 6505.
(13) Tanaka, H.; Fukumori, K.; Nishi, T. *J. Chem. Phys.* **1988**, *89*, 3363.
(14) Gusev, D. G.; Lozinsky, V. I.; Bakhmutov, V. I. *Eur. Polym. J.* **1993**, *29*, 49.
(15) Gopalsami, N.; Foster, G. A.; Dieckman, S. L.; Ellingson, W. A.; Botto, R. E. *Review of Progress in Quantitative Nondestructive Evaluation*; Thompson, D. O., Climenti, D. E., Eds.; Plenum Press: New York, 1990; Vol. 9A, p 861.
(16) Charlesby, A. *Radiat. Phys. Chem.* **1985**, *26*, 463.
(17) Harrell, J. W., Jr. *Chem. Phys. Lett.*, **1988**, *151*, 345.
(18) Harrell, J. W., Jr.; Ahuja, S. *Chem. Phys.* **1989**, *138*, 383.
(19) Douglass, D. C. *Polymer Characterization by ESR and NMR*; Woodward, A. E., Bovey, F. A., Eds.; ACS Symposium Series 142; American Chemical Society: Washington, DC, 1980.
(20) Garces, F. O.; Sivadasan, K.; Somasundaran, P.; Turro, N. J. *Macromolecules* **1994**, *27*, 272.

MA960216E